The response of anisotropic turbulence to rapid homogeneous one-dimensional compression

Krishnan Mahesh, Sanjiva K. Lele,[a] and Parviz Moin[b]
Department of Mechanical Engineering, Stanford University, Stanford, California 94305

(Received 16 March 1993; accepted 6 July 1993)

Homogeneous rapid distortion theory is used to study the response of shear flows and axisymmetric turbulence to rapid one-dimensional compression. In the shear flow problem, both normal and oblique compressions are considered. The response of these anisotropic flows to compression is found to be quite different from that of isotropic turbulence. Upon normal compression, the amplification of the streamwise component of kinetic energy and the total kinetic energy in shear flows is higher than that in isotropic turbulence. Also, normal compression decreases the magnitude of the Reynolds shear stress by amplifying the pressure–strain correlation in the shear stress equation. Obliquity of compression (defined as the angle between the directions of shear and compression) is seen to significantly affect the evolution of the Reynolds stresses. For a range of oblique angles from $-60°$ to $60°$, the amplification of streamwise kinetic energy and total kinetic energy decrease with increasing magnitude of the oblique angle. Also, the tendency of the shear stress to decrease in magnitude is diminished upon increasing the oblique angle; for large oblique angles the shear stress amplifies. Upon compression along the axis of axisymmetry, the amplification of the streamwise component of kinetic energy is higher for contracted turbulence than for isotropic turbulence, while the amplification of the total kinetic energy is lower. The above results are interpreted in a more general framework. It is shown that the amplification of the streamwise component of kinetic energy is determined by the initial $E_{11}(\kappa_1)$ (x_1 is the direction of compression). Flows with u_1 at lower κ_1 have a lower effect of pressure during compression and hence, higher amplification of $\overline{u_1^2}$. The amplification of the total kinetic energy is determined by the initial fraction of energy along the direction of compression ($\overline{u_1^2}/q^2$) and the initial $E_{11}(\kappa_1)$. Flows with higher initial $\overline{u_1^2}/q^2$ and with u_1 at lower κ_1 have a larger amplification of q^2.

I. INTRODUCTION

The study of homogeneous turbulence subjected to one-dimensional compression is of interest in problems such as the interaction of turbulence with shock waves and the compression stroke of an internal combustion engine. These flows are characterized by the time scale of the mean distortion being much smaller than the characteristic time scale of the turbulence. As a result, rapid distortion theory (henceforth referred to as RDT) is an attractive tool for analysis of these flows. The earliest use of RDT for the analysis of turbulent flows dates back to Prandtl[1] and Taylor,[2] both of whom were interested in the passage of turbulence through a wind-tunnel contraction. A formal Reynolds stress analysis of the wind-tunnel contraction problem was developed by Ribner and Tucker[3] for axisymmetric contractions, and independently, by Batchelor and Proudman[4] for arbitrary irrotational distortions. The roots of RDT applied to flows under mean compression lie in their work. More recently, Lee[5] has performed a detailed analysis of the response of turbulence to axisymmetric strain and dilatation. Comparison of the RDT predictions to experiments[6,7] and direct numerical simulations[8] show good agreement.

The above studies assumed the turbulence to be incompressible; recent studies by Durbin and Zeman[9] and Cambon *et al.*[10] have applied RDT to the compression of compressible turbulence. While Durbin and Zeman[9] have examined the pressure fluctuations and the pressure–dilatation correlation in the limit of vanishing turbulent Mach number (nearly solenoidal turbulence), Cambon *et al.*[10] have considered finite turbulent Mach numbers and shown the negligible effect of pressure fluctuations at high turbulent Mach numbers. Once again, the RDT predictions show good agreement with the simulations of Coleman and Mansour[11] and Cambon *et al.*[10]

All the studies mentioned above assume isotropic initial conditions. However, in flows such as shock waves interacting with shear layers or wind-tunnel turbulence interacting with a shock wave, the turbulence is both anisotropic and inhomogeneous upstream of the shock. The importance of the anisotropy of the turbulence in the shock/turbulence interaction was noted by Jacquin *et al.*,[12] who performed experiments on the interaction of isotropic turbulence and a turbulent jet with shock waves. Amplification of the streamwise component of turbulent kinetic energy was higher in the jet as compared to isotropic turbulence. The anisotropy in the jet was suggested by them as a possible reason for this behavior. In this paper, we isolate the effect of the anisotropy by studying the response of anisotropic homogeneous turbulence to one-

[a]Also with the Department of Aeronautics and Astronautics, Stanford University.
[b]Also with the NASA Ames Research Center.

 1070-6631/94/6(2)/1052/11/$6.00

dimensional compression. Two kinds of initial anisotropic states are considered; those of shear flow and axisymmetric turbulence. The turbulence is assumed to be incompressible and RDT is used to study its response. Precedence in the use of RDT to examine the rapid straining of anisotropic turbulence may be found in the work of Townsend,[13] Sreenivasan and Narasimha,[14] Maxey,[15] and Cambon.[16] Details of the theoretical procedure are outlined in Sec. II, while in Secs. III and IV we describe the normal and oblique compression, respectively, of sheared turbulence. The response of axisymmetric turbulence to compression is outlined in Sec. V, and finally, the conclusions drawn from this study are summarized in Sec. VI.

II. THEORETICAL PROCEDURE

Rapid distortion theory combines linearization of the governing equations with statistical averaging to describe the statistical evolution of turbulence under rapid mean distortion. The formal development of the RDT approximation is outlined in reviews such as those by Savill[17] and Hunt and Carruthers.[18] When the time scale of the mean distortion is much smaller than that of the turbulence, then the turbulence has no time to interact with itself. This allows the neglect of all terms in the governing equations that involve viscosity or the product of fluctuations, yielding a set of evolution equations that are linear in the fluctuations. An alternative formulation,[19,20] corresponding to low Reynolds number or "weak" turbulence requires retention of the viscous terms. In this paper, we neglect the viscous terms.

Linearization of the continuity and momentum equations yields the following set of equations:

$$\frac{\partial u_i}{\partial x_i}=0, \tag{1a}$$

$$\frac{\partial u_i}{\partial t}+U_j\frac{\partial u_i}{\partial x_j}+u_j\frac{\partial U_i}{\partial x_j}=-\frac{1}{\rho}\frac{\partial p}{\partial x_i}, \tag{1b}$$

where U_i and ρ are the mean velocity and density, respectively, and u_i and p are the fluctuating velocity field and pressure, respectively. For irrotational mean distortions, it is convenient to solve the linearized vorticity equation, which reduces to Cauchy's equation.[4,5] Note that the fluctuations are assumed to be solenoidal. If the mean distortion is solenoidal, then the above equations correspond to linearization of the incompressible Navier–Stokes equations. However, if the mean field is dilatational (as for a one-dimensional compression), then the governing equations are the *compressible* Navier–Stokes equations and the above set of equations therefore describe evolution of the solenoidal component of the compressible flow field under the assumption that its evolution is independent of the dilatational component. [Alternatively, Eqs. (1a) and (1b) describe the evolution of a compressible flow field with spatially uniform but time-dependent density.[5]] The solenoidal and dilatational component are coupled, even in the linear limit, for rotational mean flows.[21] However, for irrotational mean distortions, the solenoidal component may be assumed to evolve independently in the limit $\Delta m=\Gamma_0 L/a\ll 1$, where, Γ_0 is the mean strain rate, L is a turbulence length scale, and a is the mean speed of sound; i.e., the turbulence is nearly incompressible.[10]

The assumption of homogeneity constrains the mean velocity gradient to be uniform; i.e., the mean velocity is of the form $U_i=A_{ik}(t)x_k$. For incompressible turbulence, this is the only requirement for homogeneity; since, as discussed above, we consider evolution of the solenoidal component of a compressible flow field, we constrain the mean field to satisfy homogeneity for compressible turbulent fluctuations. As a result, in addition to a uniform velocity gradient, the mean field satisfies the compressible Euler equations and has uniform pressure and density.[21]

The procedure for solution of Eqs. (1a) and (1b) is fairly well established. One method of solution[4] involves using a Fourier representation where the wave number changes with time as

$$u_i(\mathbf{x},t)=\sum_{\mathbf{k}}\hat{u}_i(\mathbf{k},t)e^{ik_j(t)x_j},$$

$$p(\mathbf{x},t)=\sum_{\mathbf{k}}\hat{p}(\mathbf{k},t)e^{ik_j(t)x_j},$$

where

$$\frac{dk_\alpha}{dt}+k_j A_{j\alpha}=0. \tag{2}$$

An alternative equivalent method of solution[22] is to transform coordinates to a system that deforms with the mean field; i.e.,

$$\xi_i=B_{ik}(t)x_k,\quad \tau=t,$$

where

$$\frac{d}{dt}B_{nk}+A_{jk}B_{nj}=0. \tag{3}$$

The transformed equations are then solved using conventional Fourier representation. Knowledge of the Fourier coefficients enables computation of the energy spectrum tensor, which is then integrated over all wave numbers to determine the Reynolds stresses.

Homogeneous RDT requires specification of the initial energy spectrum. As mentioned previously, earlier studies assume an isotropic initial spectrum. This paper differs, in that the compression of anisotropic turbulence is considered. Details of the analysis are presented in the following sections.

III. NORMAL COMPRESSION OF SHEARED TURBULENCE

A. Problem formulation

In this section, we formulate the problem of sheared turbulence that is suddenly subjected to normal compression. We first note that one-dimensional homogeneous compression is characterized by the following mean field:

$$U_1=\frac{\Gamma_0}{1+\Gamma_0 t}x_1,\quad U_2=U_3=0, \tag{4a}$$

$$\rho=\frac{\rho_0}{1+\Gamma_0 t}, \tag{4b}$$

$$P=\frac{P_0}{(1+\Gamma_0 t)^{\gamma}}, \tag{4c}$$

where U_1, U_2, and U_3 are the mean velocity components in the x_1, x_2, and x_3 directions, respectively; ρ and P are the mean density and pressure, respectively, and are uniform in space. Here Γ_0 is negative for compression and positive for expansion.

We consider isotropic turbulence that is subjected to rapid homogeneous shear, i.e.,

$$U_1=S_0 x_2, \quad \rho=\rho_0, \quad P=P_0. \tag{5}$$

At a nondimensional time $\beta_0=S_0 t_0$ during application of shear, we introduce the one-dimensional compression, i.e., for $t>t_0$,

$$U_1=\frac{\Gamma_0}{1+\Gamma_0(t-t_0)} x_1+\frac{S_0}{1+\Gamma_0(t-t_0)} x_2, \tag{6a}$$

$$\rho=\frac{\rho_0}{1+\Gamma_0(t-t_0)}, \tag{6b}$$

$$P=\frac{P_0}{[1+\Gamma_0(t-t_0)]^{\gamma}}. \tag{6c}$$

The shear rate changes with time during the application of compression to satisfy the compressible Euler equations. Note that the shear is along x_2 while the compression is along x_1; we term this normal compression.

Under RDT, the state of turbulence before compression is dependent upon the total shear β_0; its subsequent evolution depends upon β_0, the ratio of shear rate to the rate of compression (S_0/Γ_0) and the total volumetric strain (ρ/ρ_0). Since our interest is in the compression of anisotropic turbulence, we consider the regime where the shear sets up the initial anisotropic field and is negligible, as compared to the subsequently applied compression; i.e., $S_0/\Gamma_0 \ll 1$. In this paper, S_0/Γ_0 is -0.1 for all cases presented. Lower values of S_0/Γ_0 (for, e.g., $S_0/\Gamma_0=-0.01$) yielded results identical to those shown here. Thus, we effectively consider the rapid one-dimensional compression of sheared turbulence. Figure 1 shows a schematic of the straining process.

Regarding the solution of the RDT equations, our strategy was to transform coordinates to a system that deformed with the mean field. Using Fourier representation in the transformed coordinates, we derived equations describing the evolution of the energy spectrum tensor that were numerically advanced in time. At each time step, the energy spectrum tensor was numerically integrated over all wave numbers to obtain the Reynolds stresses. As indicated above, until time t_0 the mean field is pure shear. The RDT equations for pure shear have been solved analytically,[23,24] and hence we do not give the evolution equations for the energy spectrum tensor. We only note that the coordinate transform used is as follows:

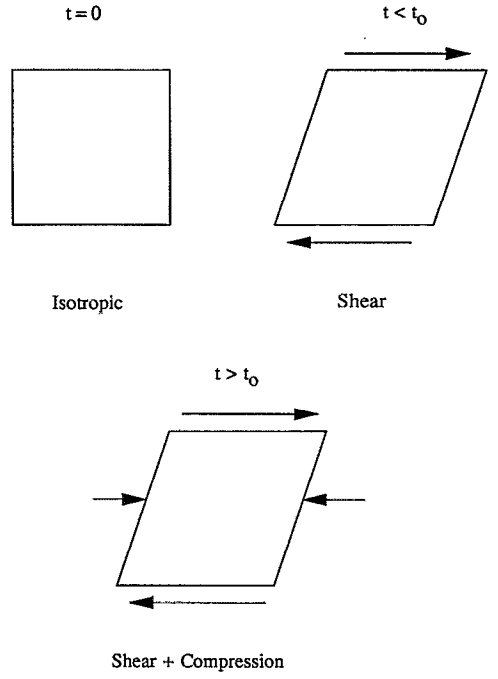

FIG. 1. Schematic of the normal compression of a shear flow.

$$\xi_1=x_1-S_0 t x_2, \quad \xi_2=x_2, \quad \xi_3=x_3, \quad \tau=t. \tag{7}$$

At time $t_0=\beta_0/S_0$, the coordinate transformation changes to accommodate the compression. The new transformation is given by

$$\xi_1=\frac{x_1}{1+\Gamma_0(t-t_0)}-[\beta_0+S_0(t-t_0)]x_2,$$
$$\xi_2=x_2, \quad \xi_3=x_3, \quad \tau=t. \tag{8}$$

For $t>t_0$, the RDT equations are transformed to the above coordinate system. Using the Fourier representation,

$$u_i(\boldsymbol{\xi},\tau)=\sum_{\boldsymbol{\kappa}} \hat{u}_i(\boldsymbol{\kappa},\tau) e^{i\kappa_j \xi_j}, \tag{9a}$$

$$p(\boldsymbol{\xi},\tau)=\sum_{\boldsymbol{\kappa}} \hat{p}(\boldsymbol{\kappa},\tau) e^{i\kappa_j \xi_j}, \tag{9b}$$

the RDT equations take the following form for $t>t_0$:

$$\frac{d\hat{u}_1}{d\tau}=-\frac{\Gamma_0}{1+\Gamma_0(\tau-\tau_0)}\hat{u}_1-\frac{S_0}{1+\Gamma_0(\tau-\tau_0)}\hat{u}_2 + \frac{\kappa_1}{1+\Gamma_0(\tau-\tau_0)}\left(\frac{i\hat{p}}{\rho}\right), \tag{10a}$$

$$\frac{d\hat{u}_2}{d\tau}=\left(\kappa_2-\frac{S_0(\tau-\tau_0)}{1+\Gamma_0(\tau-\tau_0)}\kappa_1\right)\left(\frac{i\hat{p}}{\rho}\right), \tag{10b}$$

$$\frac{d\hat{u}_3}{d\tau}=\kappa_3\left(\frac{i\hat{p}}{\rho}\right), \tag{10c}$$

$$\left(\frac{i\hat{p}}{\rho}\right)=\frac{[\kappa_1\Gamma_0/(1+\Gamma_0(\tau-\tau_0))]\hat{u}_1+[\kappa_1 S_0-\kappa_2\Gamma_0+\kappa_1 S_0/(1+\Gamma_0(\tau-\tau_0))]\hat{u}_2-\kappa_3\Gamma_0\hat{u}_3}{\kappa_1^2[1+S_0^2(\tau-\tau_0)^2]/(1+\Gamma_0(\tau-\tau_0))-2\kappa_1\kappa_2 S_0(\tau-\tau_0)+(\kappa_2^2+\kappa_3^2)[1+\Gamma_0(\tau-\tau_0)]}. \tag{10d}$$

Note that the equations describing the evolution for $t<t_0$ (Pure shear) may be obtained by substituting $\Gamma_0=0$ in Eqs. (10a)–(10d). The RDT equations for a pure compression allow analytical solution, as do the equations for pure shear. However, as seen above, the combination of shear and compression yields a formidable set of equations that we have not been able to solve analytically. Instead, Eqs. (10a)–(10d) were used to derive evolution equations for the energy spectrum tensor $E_{ij}(\kappa,\tau)$, defined as $E_{ij}=\hat{u}_i\hat{u}_j^*$, where the superscript "*" refers to the complex conjugate. For reasons of brevity, the equation for E_{ij} is not reproduced here; it has the following form:

$$\frac{dE_{ij}}{d\tau}=C_{il}E_{lj}+C_{jl}E_{li}. \tag{11}$$

The above system of equations is integrated numerically to compute $E_{ij}(\kappa,\tau)$. Here E_{ij} is then integrated over all wave numbers to compute the Reynolds stress tensor $R_{ij}(\tau)$ defined as $R_{ij}=\overline{u_iu_j}$; i.e.,

$$R_{ij}(\tau)=\int E_{ij}(\kappa,\tau)d^3\kappa. \tag{12}$$

The integration is carried out in polar coordinates,

$$\kappa_1=\kappa\cos\phi,\quad \kappa_2=\kappa\sin\phi\cos\theta,$$

$$\kappa_3=\kappa\sin\phi\sin\theta,\quad d^3\kappa=\kappa^2\sin\phi\,d\phi\,d\theta\,d\kappa,$$

where κ varies from 0 to ∞; ϕ, from 0 to π; and θ, from 0 to 2π. Note that since at $\tau=0$, the energy spectrum tensor is assumed to be isotropic; i.e.,

$$E_{ij}(\kappa,0)=\frac{E(\kappa)}{4\pi\kappa^2}\left(\delta_{ij}-\frac{\kappa_i\kappa_j}{\kappa^2}\right),$$

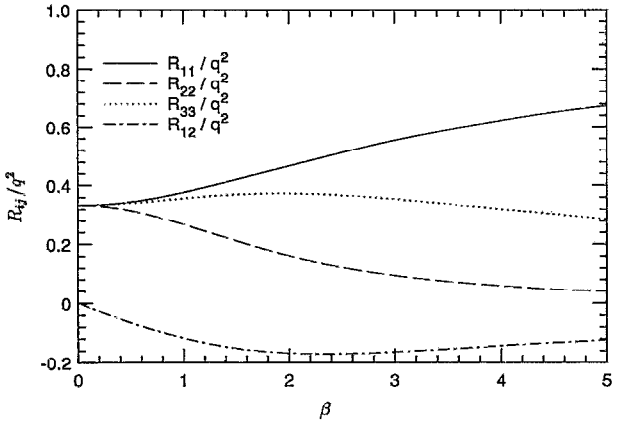

FIG. 2. Evolution of R_{ij}/q^2 as predicted by RDT applied to the homogeneous shear of initially isotropic turbulence.

it can be shown that $R_{ij}(\tau)$ is independent of the initial three-dimensional energy spectrum tensor $E(\kappa)$ and the magnitude of the wave number vector.

B. Results

In this section, we present results of the analysis described in the previous section. As mentioned, we are effectively examining the effects of normal compression on sheared turbulence. Regarding the use of RDT to obtain the energy spectrum tensor that characterizes a shear flow, we refer to Townsend,[25] where the RDT predictions of Reynolds stress correlations, spectra, and nondimensional Reynolds stresses were compared to experiment, and good agreement was observed.

The evolution of R_{ij}/q^2 ($q^2=R_{ll}$ is the trace of the Reynolds stress tensor), as predicted by RDT applied to the rapid shear of initially isotropic turbulence is shown in Fig. 2. The quantity plotted on the abscissa is the total shear β defined as $\beta=S_0 t$. Note that after a moderate amount of total shear (β between 2 and 3), the nondimensional Reynolds stresses are quite close to values obtained in shear flows, such as homogeneous shear flow, turbulent channel flow,[26] and boundary layers.[25] For example, in homogeneous shear flow,[26] R_{11}/q^2, R_{22}/q^2, R_{33}/q^2, and R_{12}/q^2 are 0.54, 0.16, 0.31, and 0.14, respectively. For a total shear of 2.5, RDT yields values of 0.51, 0.12, 0.36, and 0.16, respectively. The good agreement of the nondimensional Reynolds stresses suggests that the large eddies in turbulent shear flows have very nearly the shape suggested by RDT.[25] This conclusion is further supported by direct numerical simulations by Lee *et al.*[27] of turbulence subjected to very high shear rates, where structures similar to near wall "streaks" were observed.

Next, we examine the evolution of this sheared turbulence upon compression. Here q^2 normalized with its value at the start of compression is plotted against the total volumetric strain in Fig. 3, where the different curves correspond to different values of total initial shear (β_0). Here $\beta_0=0$ corresponds to the compression of initially isotropic turbulence. We see that q^2 is amplified upon compression, with the amplification ratio increasing as the initial total shear increases. The amplification of turbulent kinetic energy upon normal compression is thus higher for a shear flow than it is for isotropic turbulence. The evolution of the components of turbulent kinetic energy is shown in Fig. 4, where β_0 was set to 3. All three components amplify with the x_1 (direction of compression) component being amplified the most. The reason for the preferential amplification of the x_1 component is due to the fact that it is directly "produced" by the compression, while the other components amplify through the redistributive nature of the pressure–strain correlation in the Reynolds stress equations. To gauge the importance of the initial anisotropy on

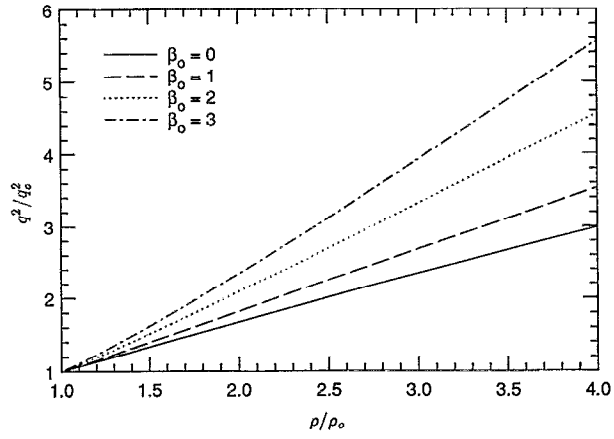

FIG. 3. Evolution of q^2 upon the normal compression of sheared turbulence. The different curves correspond to different values of initial total shear.

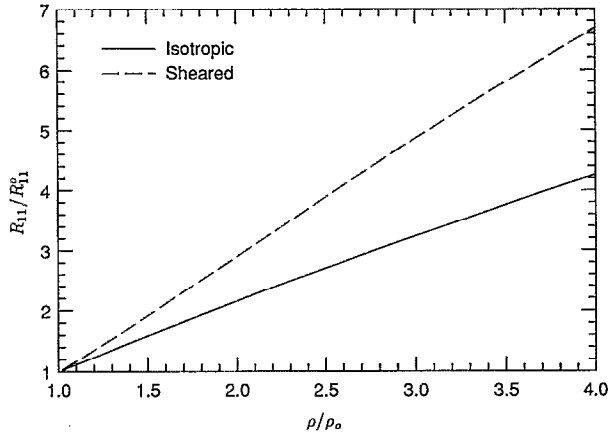

FIG. 5. Comparison of the amplification of R_{11} of sheared turbulence ($\beta_0=3$) to that of isotropic turbulence.

the amplification of $\overline{u_1^2}$, we compare the amplification of $\overline{u_1^2}$ in initially sheared turbulence with that in initially isotropic turbulence (Fig. 5). Note that the amplification of $\overline{u_1^2}$ in the shear flow is much higher than that in isotropic turbulence. For example, at a density ratio of 3, the amplification ratio is 3.4 for initially isotropic turbulence and 4.85 for initially sheared turbulence—an increase of about 43%.

As mentioned earlier, shear flows in equilibrium are characterized by typical values of R_{ij}/q^2. It is of interest to see how these values change upon normal compression. Figure 6 shows the the diagonal terms of the tensor. Compression increases the contribution of u_1 to the turbulent kinetic energy while decreasing that of u_2 and u_3. We also note (over the range of total volumetric strain shown) that the ordering of kinetic energy components ($u_1 > u_3 > u_2$) is retained upon normal compression.

The Reynolds shear stress $R_{12} = \overline{u_1 u_2}$ is an important quantity in shear flows. Figure 7 shows the evolution of R_{12}/q^2 upon compression. The three curves correspond to different values of total initial shear. We see that upon normal compression, R_{12}/q^2 decreases in magnitude, and for sufficiently large total volumetric strains, it changes sign. This trend was first observed by Cambon,[16] and is hastened upon increasing the initial total shear. We investigate the cause of this behavior by examining the terms in the Reynolds shear stress equation. The evolution equation for R_{12} is

$$\frac{d}{dt}R_{12} = -\frac{\Gamma_0}{1+\Gamma_0 t}R_{12} - \frac{S_0}{1+\Gamma_0 t}R_{22} + \pi_{12}, \qquad (13)$$

where π_{ij} is the pressure–strain correlation defined as $\pi_{ij} = \overline{p(u_{i,j}u_{j,i})}/\rho$. Note that both the strain and shear production terms tend to increase the magnitude of R_{12} (make it more negative). The tendency of $|R_{12}|$ to decrease must therefore be due to the pressure strain correlation. Figure 8 illustrates the evolution of terms in the budget of R_{12} for the case with $\beta_0=3$. We see that the tendency of R_{12} to decrease upon normal compression is due to amplification of the pressure–strain correlation and the consequent upsetting of the initial balance between "production" and the pressure–strain correlation in the shear flow.

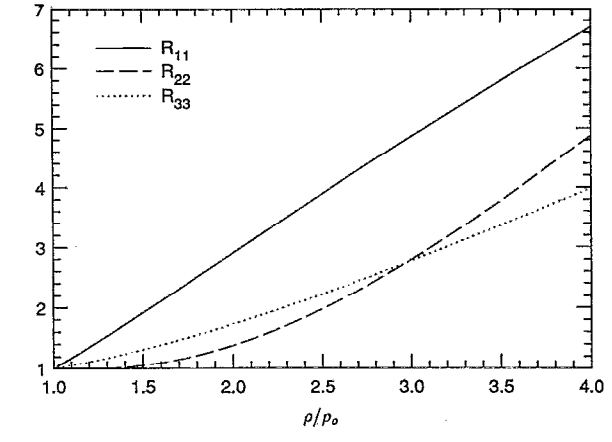

FIG. 4. Evolution of the components of turbulent kinetic energy when sheared turbulence ($\beta_0=3$) is subjected to normal compression.

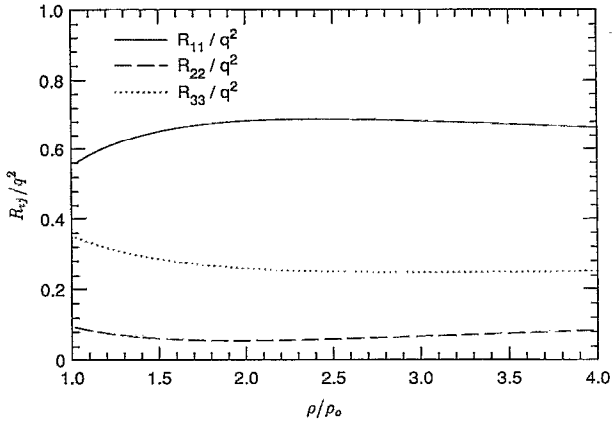

FIG. 6. Evolution of the diagonal terms of R_{ij}/q^2 when sheared turbulence ($\beta_0=3$) is subjected to normal compression.

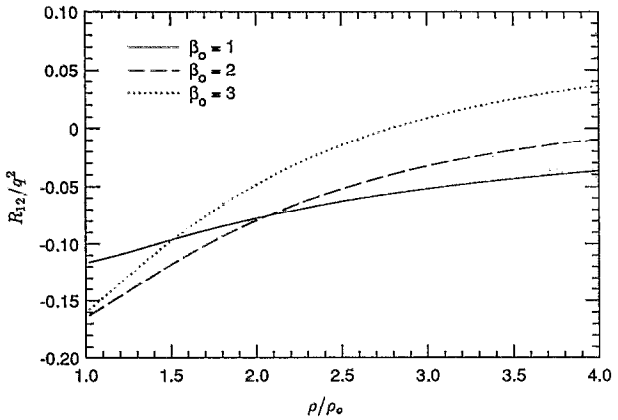

FIG. 7. Evolution of R_{12}/q^2 when sheared turbulence is subjected to normal compression. The different curves correspond to different values of initial total shear.

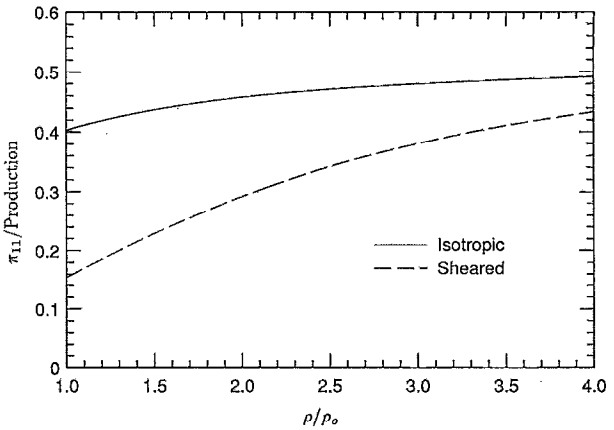

FIG. 9. Evolution of the ratio of π_{11} to the production term in the R_{11} equation upon normal compression. The compression of sheared turbulence ($\beta_0=3$) is compared to that of isotropic turbulence.

C. Interpretation of the results

We have seen that the response of a shear flow to normal compression is quite different from that of isotropic turbulence. A noticeable feature is the higher amplification of $\overline{u_1^2}$ and q^2 in the shear flow. In this section, we attempt to explain this observation by posing the following question: "What aspect of the initial anisotropic field is important in determining the evolution of kinetic energy during a one-dimensional compression?"

The evolution equations for $\overline{u_1^2}$ and q^2 during rapid compression are given by

$$\frac{d\overline{u_1^2}}{d\tau} = -2\frac{\Gamma_0}{1+\Gamma_0\tau}\overline{u_1^2} + \pi_{11}, \tag{14a}$$

$$\frac{dq^2}{d\tau} = -2\frac{\Gamma_0}{1+\Gamma_0\tau}\overline{u_1^2}. \tag{14b}$$

The pressure–strain correlation "takes" energy from $\overline{u_1^2}$ and redistributes it among the other components. The amplification of $\overline{u_1^2}$, and hence q^2 through Eq. (14b), would increase if the pressure–strain correlation were to decrease. Also, since in the RDT limit the pressure–strain correlation is the only term in the budget apart from the production term, a higher amplification rate automatically implies a lower pressure–strain correlation. The relative magnitude of the pressure–strain term in the energy budget may be gauged from its short time behavior. It is easily shown that in turbulence subjected to rapid one-dimensional compression, π_{11} evolves as

$$\pi_{11} = -2\Gamma_0 c \int \frac{c^2\kappa_1^2}{c^2\kappa_1^2+\kappa_2^2+\kappa_3^2} E_{11}(\kappa)d^3\kappa, \tag{15}$$

where $c=\rho/\rho_0$. Thus π_{11} strongly depends upon the spectral distribution of the u_1 component of velocity. Note that as the energy distribution in u_1 moves to smaller κ_1, the magnitude of π_{11} decreases. The small time evolution of π_{11} may be estimated by replacing E_{11} in Eq. (15) with its initial value, E_{11}^0. This small time evolution shows how the spectral distribution of u_1 in the initial field affects the rate of change of $\overline{u_1^2}$ when anisotropic turbulence is compressed.

Since mean shear tends to stretch the turbulence in the streamwise direction, $\hat{u}_1$ in a shear flow has energy at smaller κ_1, as compared to isotropic turbulence, and hence according to Eq. (15), a lower initial value of π_{11}. This is shown in Fig. 9, where the ratio of π_{11} to the production term in the R_{11} equation is plotted. The pressure–strain correlation is indeed seen to play a smaller role when shear flow is compressed. As one continues the compression, the energy in u_1 is moved to larger κ_1, and hence the pressure–strain correlation would progressively become more important. In the limit of infinite ρ/ρ_0, the ratio of π_{11} to production is independent of the initial energy spectrum; it is equal to 1. For turbulence subjected to one-dimensional compression, under RDT,

$$E_{11}(\kappa) = \frac{c^2 E_{11}^0(\kappa)}{c^2(\kappa_1/\kappa)^2+(\kappa_2/\kappa)^2+(\kappa_3/\kappa)^2}, \tag{16}$$

where $c=\rho/\rho_0$.

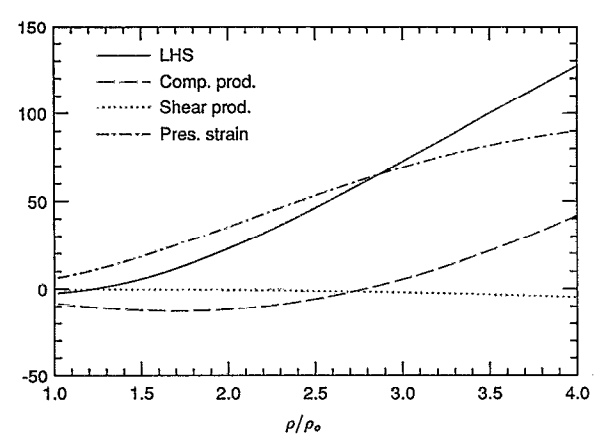

FIG. 8. Budget of terms in the R_{12} evolution equation during the normal compression of sheared turbulence ($\beta_0=3$). Time is nondimensionalized by Γ_0 and the Reynolds stresses by R_{12}^0.

Denoting the denominator in the above expression by D, the rate of change of E_{11} is given by

$$\frac{dE_{11}}{d\tau}=\frac{E_{11}^0}{D^2}\left(D\frac{dc^2}{d\tau}-c^2\frac{dD}{d\tau}\right). \tag{17}$$

Noting that $dc/dt=-\Gamma_0 c^2$ and considering very large compressions, it can be shown that

$$\lim_{c\to\infty}\frac{dE_{11}}{d\tau}=0. \tag{18}$$

Since E_{11} when integrated over all wave numbers yields R_{11}, the above equation implies that in the limit of very large c, $d\overline{u_1^2}/d\tau = 0$. Substitution into Eq. (14a) shows that asymptotically, π_{11}=production. Note that this relation is independent of the initial energy spectrum. The asymptotic behavior shows the diminishing effect of initial anisotropy upon the pressure–strain correlation as time progresses. This is supported by Fig. 9, where the two curves tend toward each other as c increases.

We see that when anisotropic turbulence is compressed (in the x_1 direction), the feature of the initial field that determines kinetic energy evolution is $E_{11}^0(\kappa_1)$. As the energy in u_1^0 moves to smaller κ_1, the relative importance of π_{11} decreases, resulting in larger amplification of $\overline{u_1^2}$. The amplification of q^2, in addition to being influenced by E_{11}^0, is also influenced by the initial value of $\overline{u_1^2}/q^2$. The kinetic energy equation for a one-dimensional compression [Eq. (14b)] may be rewritten as

$$\frac{1}{2q_0^2}\frac{dq^2}{d\tau}=-\frac{\Gamma_0}{1+\Gamma_0\tau}\left(\frac{\overline{u_1^2}}{\overline{u_1^{02}}}\right)\left(\frac{\overline{u_1^{02}}}{q_0^2}\right). \tag{19}$$

Note that as $\overline{u_1^{02}}/q_0^2$ increases, the amplification of q^2 increases. This explains the trend seen in Fig. 3. In addition to having energy at lower κ_1, a shear flow that is subjected to normal compression also has a larger fraction of its energy along the direction of compression, resulting in a higher amplification of q^2, as compared to isotropic turbulence.

Thus far, we have examined the effect of compression on sheared turbulence normal to the direction of shear. Since shear flows are anisotropic, one would expect the direction of compression relative to the shear to be an important parameter; i.e., the oblique compression of a shear flow would yield results different from normal compression. In the section that follows, we discuss the procedure and results of RDT applied to the problem of oblique compression.

IV. OBLIQUE COMPRESSION OF SHEARED TURBULENCE

A. Problem formulation

Under RDT, the obliquity of compression may be characterized by the angle θ between the direction of compression and the direction of the upstream shear flow. Note that $\theta=0$ corresponds to the normal compression discussed in the previous section. Recall that the normal compression problem was formulated by considering sheared turbulence subjected to simultaneous shear and compression in the regime, where the compression rate was much higher than the rate of shear. The sole reason for retention of the shear during compression was to avoid the destruction of vorticity. However, one might adopt the point of view that if the mean shear is not important during the process of compression, then it may be ignored, except for its effect on the initial spectrum. This is the approach adopted in this section in applying RDT to the oblique compression of sheared turbulence. We essentially repeat RDT for turbulence subjected to a one-dimensional compression. However, the initial energy spectrum instead of being isotropic is the RDT solution to isotropic turbulence subjected to homogeneous shear. Also, as mentioned, the initial mean shear is assumed to be at angle θ to the subsequently applied compression. The validity of this approach was verified by comparison of the results for $\theta=0$ to the more completely formulated normal compression problem.

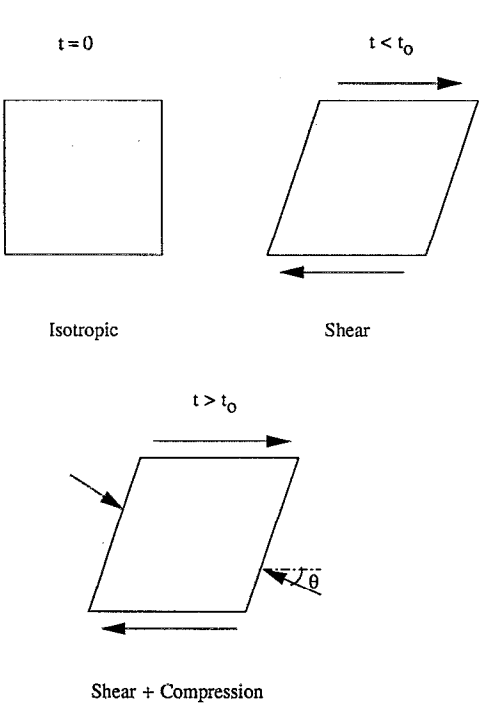

FIG. 10. Coordinate system used in the analysis of the oblique compression of sheared turbulence.

Figure 10 shows a schematic of the the oblique compression problem. Note that the shear is assumed to be in the x_2 direction. For reasons of convenience, the time-dependent wave number approach[4] was used to solve the RDT equations. The RDT solution to the oblique compression problem requires knowledge of the evolution of the energy spectrum tensor when isotropic turbulence is subjected to homogeneous shear and the transfer function of the vorticity spectrum tensor when turbulence (not necessarily isotropic) is subjected to a one-dimensional compression. As indicated earlier, these problems have been solved analytically. Assuming knowledge of these transfer

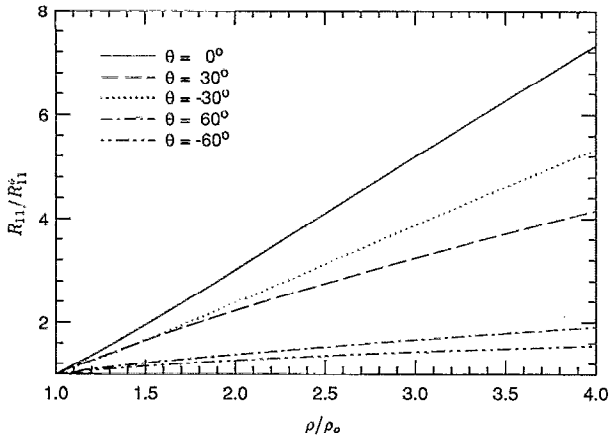

FIG. 11. Evolution of R_{11} upon the oblique compression of sheared turbulence ($\beta_0=3$). The different curves correspond to different values of the oblique angle.

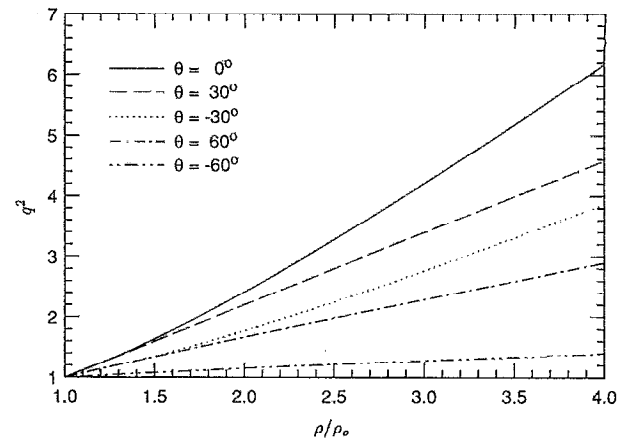

FIG. 12. Evolution of q^2 upon the oblique compression of sheared turbulence ($\beta_0=3$). The different curves correspond to different values of the oblique angle.

functions, the procedure for RDT applied to the oblique compression problem is as follows.

(1) Consider isotropic turbulence that is subjected to homogeneous shear in the x_2 direction. Denote the wave number vector at $t=0$ by $\mathbf{k}_0$. For a given total shear (defined in the previous section) compute the energy spectrum tensor at the end of shear.

(2) With reference to Fig. 10, rotate the energy spectrum tensor and the wave number vector by the angle θ. This aligns the field with the compression.

(3) From the rotated energy spectrum tensor and the wave number vector, obtain the vorticity spectrum tensor in the rotated coordinates.

(4) Using the transfer functions for the compression problem, obtain the vorticity spectrum tensor and wave number vector after compression.

(5) Using the inverse of the relation in (3) above, obtain the energy spectrum tensor after compression in the rotated coordinates. Integrate the energy spectrum tensor over $\mathbf{k}_0$ to obtain the Reynolds stress tensor in rotated coordinates.

(6) Rotate the Reynolds stress tensor back by the angle θ. This yields the Reynolds stress tensor after compression in the original coordinate system.

B. Results

In this section we describe some of the results of RDT applied to the oblique compression of sheared turbulence. The effect of the oblique angle θ is gauged by comparison to the previously discussed normal compression problem. The amplification of the streamwise component of turbulent kinetic energy upon compression is shown in Fig. 11 for different angles of obliquity.

The initial condition corresponds to sheared turbulence with $\beta_0=3$. Recall that $\theta=0$ corresponds to normal compression. Note the decrease in amplification ratio with increasing magnitude of the oblique angle. The effect of oblique compression on q^2 is shown in Fig. 12. Once again, the amplification of q^2 decreases as the oblique angle increases. In the previous section, we emphasized the importance of $E_{11}(\kappa_1)$ and $\overline{u_1^2}/q^2$ on the amplification of kinetic energy. If oblique compression is viewed in a coordinate system aligned with the compression, we see that the effect of oblique compression may be explained by the initial value of $E_{\theta\theta}(\kappa_\theta)$ and $\overline{u_\theta^2}/q^2$, where θ refers to the direction of compression.

In the previous section, we noted how normal compression could significantly change the nondimensional Reynolds stresses of a shear flow. The effect of oblique compression on the diagonal elements of R_{ij}/q^2 is shown in Figs. 13–15. It is clear that obliquity of compression has a significant effect on the evolution of the Reynolds stresses. The qualitative difference in the curves for different oblique angles is striking to note. This indicates the importance of the direction of compression in interpreting experiments on shock/turbulence interaction.

Figure 16 shows the evolution of the nondimensional Reynolds shear stress upon oblique compression. Recall the effect of normal compression to decrease R_{12}/q^2 and

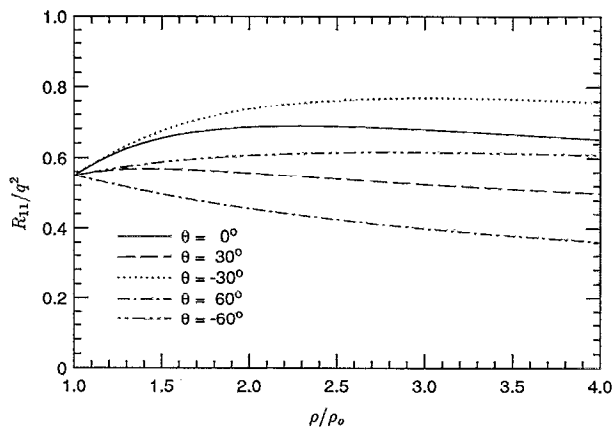

FIG. 13. Evolution of R_{11}/q^2 upon the oblique compression of sheared turbulence ($\beta_0=3$). The different curves correspond to different values of the oblique angle.

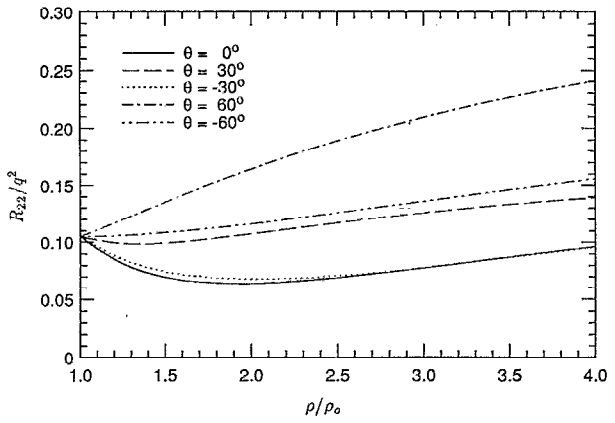

FIG. 14. Evolution of R_{22}/q^2 upon the oblique compression of sheared turbulence ($\beta_0=3$). The different curves correspond to different values of the oblique angle.

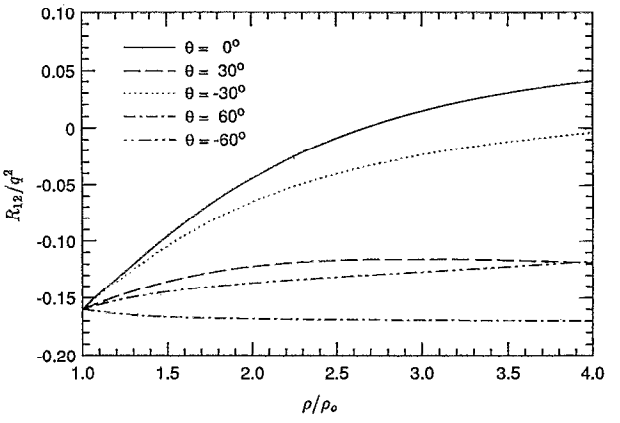

FIG. 16. Evolution of R_{12}/q^2 upon the oblique compression of sheared turbulence ($\beta_0=3$). The different curves correspond to different values of the oblique angle.

even change its sign. In comparison, we see that this trend decreases as the compression becomes more oblique and for large oblique angles, R_{12}/q^2 slightly amplifies.

V. COMPRESSION OF AXISYMMETRIC TURBULENCE ALONG THE AXIS OF AXISYMMETRY

In this section, we consider the compression of axisymmetric turbulence along the axis of axisymmetry. A corresponding physical situation would be that of grid turbulence interacting with a normal shock after passing through a wind-tunnel contraction. Our interest is in seeing how the response of axisymmetric turbulence to compression is different from that of isotropic turbulence and to verify the conclusions drawn from the shear flow problem regarding the effect of initial anisotropy.

A schematic of the problem is shown in Fig. 17. To generate axisymmetric turbulence, isotropic turbulence is subjected to rapid homogeneous axisymmetric strain; i.e.,

$$U_1=\alpha x_1, \quad U_2=-\frac{\alpha}{2}x_2, \quad U_3=-\frac{\alpha}{2}x_3, \quad \rho=\rho_0, \tag{20}$$

where U_1, U_2, and U_3 are the mean velocity components in the x_1, x_2, and x_3 directions, respectively, and ρ is the mean density, which is uniform. Here $\alpha>0$ corresponds to axisymmetric contraction, while $\alpha<0$ corresponds to axisymmetric expansion. The above strain is applied until the nondimensional time αt_0 when it is replaced by the one-dimensional compression given by Eqs. (4a)–(4c). Axisymmetrically strained turbulence is thus the initial condition for the one-dimensional compression. RDT is used to obtain the energy spectrum tensor at the end of axisym-

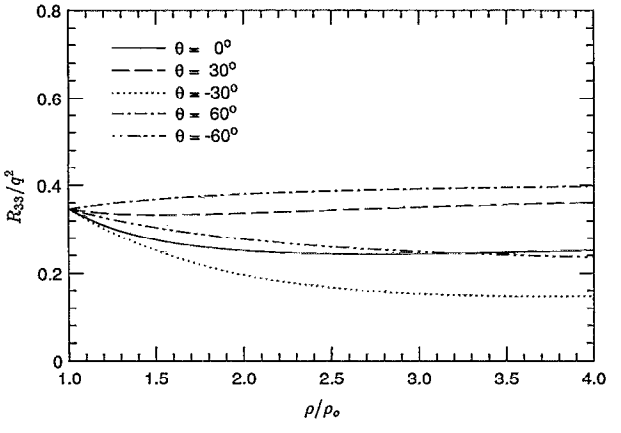

FIG. 15. Evolution of R_{33}/q^2 upon the oblique compression of sheared turbulence ($\beta_0=3$). The different curves correspond to different values of the oblique angle.

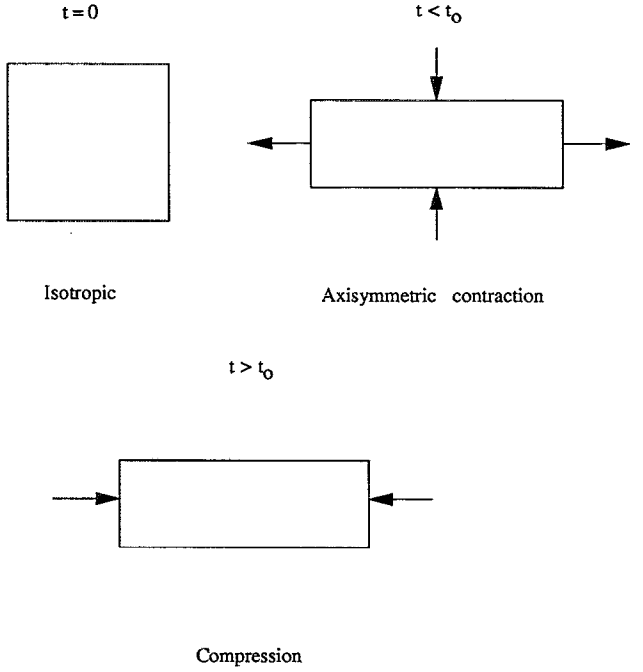

FIG. 17. Schematic of the normal compression of axisymmetric turbulence.

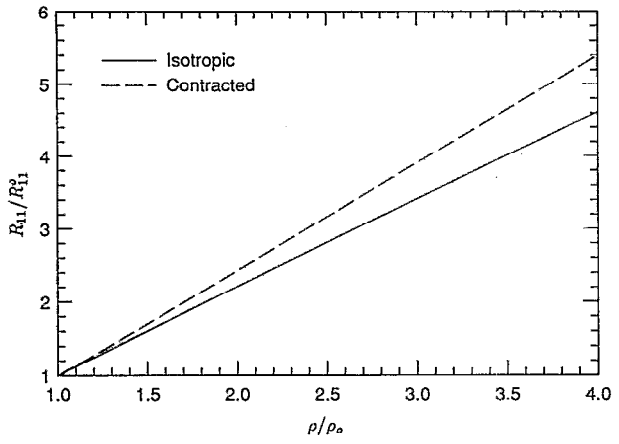

FIG. 18. Comparison of the amplification of R_{11} of isotropic turbulence to that of axisymmetrically contracted turbulence.

metric straining. This energy spectrum tensor is then used as the initial condition for the one-dimensional compression.

Regarding the nature of turbulence subjected to axisymmetric strain, as mentioned earlier, Lee[5] has done an extensive analysis of the problem using RDT. As a result, we do not reproduce the equations for the energy spectrum tensor; we just mention that while contraction suppresses streamwise fluctuations (decreases $\overline{u_1^2}/q^2$) and moves the energy distribution in u_1 to small κ_1 ("rod-like" structures), expansion amplifies streamwise velocity fluctuations (increases $\overline{u_1^2}/q^2$) and moves the energy in u_1 to large κ_1 ("disk-like" structures). Further details may be found in Lee.[5]

Next we examine the evolution of axisymmetric turbulence upon compression. In the shear flow problem, we noted that a flow with u_1 at lower κ_1 would have a lesser influence of pressure, and hence a higher amplification of $\overline{u_1^2}$. With respect to axisymmetric turbulence, this would imply that the amplification of $\overline{u_1^2}$ of turbulence that is passed through an axisymmetric contraction would be higher than that of isotropic turbulence. We compare in Fig. 18 the amplification of $\overline{u_1^2}$ of contracted turbulence ($\alpha t_0 = 0.5$) to that of isotropic turbulence and see that this behavior is reproduced. The amplification of q^2 is plotted in Fig. 19, where the two curves correspond to initially isotropic turbulence and contracted turbulence, respectively. Recall that the parameters influencing the amplification were identified as $E_{11}^0(\kappa_1)$ and the initial value of $\overline{u_1^2}/q^2$. In axisymmetrically contracted turbulence, although u_1 is at lower κ_1, the initial value of $\overline{u_1^2}/q^2$ is lower. Therefore, there is a competition between these two parameters in determining the net amplification of q^2. From Fig. 19, we see that the lower value of $\overline{u_1^2}/q^2$ dominates, resulting in the contracted turbulence having a lower amplification of q^2.

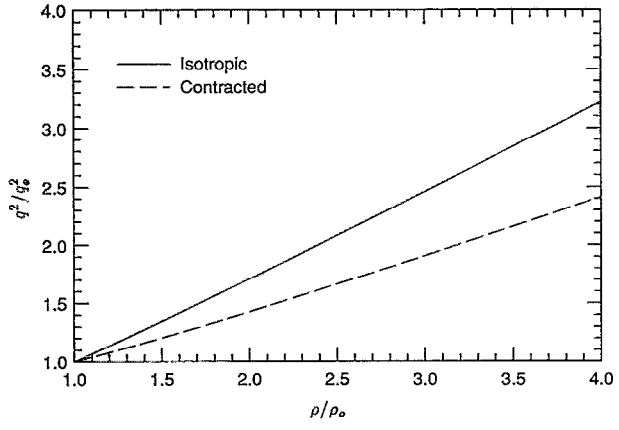

FIG. 19. Comparison of the amplification of q^2 of isotropic turbulence to that of axisymmetrically contracted turbulence.

VI. CONCLUSIONS

Homogeneous rapid distortion theory was used to examine the response of incompressible, anisotropic turbulence to a rapid one-dimensional compression. Two problems were studied—the compression of sheared turbulence and the compression of axisymmetric turbulence along the axis of axisymmetry. In the shear flow problem, both normal and oblique compressions (with respect to the shear) were considered. The response of these anisotropic flows to compression is found to be quite different from the previously studied, compression of isotropic turbulence. The differences are interpreted in a more general framework and the relevant parameters influencing kinetic energy amplification are identified.

Here, $E_{11}(\kappa_1)$ of the initial field is found to determine the evolution of the streamwise (the direction of compression) component of kinetic energy. Flows with u_1 at lower κ_1 have a reduced effect of pressure during compression, and hence a higher amplification of u_1. The evolution of q^2 upon compression is influenced by the initial fraction of kinetic energy in the direction of compression ($\overline{u_1^2}/q^2$), in addition to the initial $E_{11}(\kappa_1)$. Flows with a larger value of initial $\overline{u_1^2}/q^2$ and u_1 at lower κ_1 have a larger amplification of q^2.

Upon normal compression, all components of turbulent kinetic energy of sheared turbulence are amplified, with the streamwise component being amplified the most. The amplification of $\overline{u_1^2}$ and q^2 is higher than that in isotropic turbulence. Normal compression decreases the turbulent shear stress and for large enough compressions changes its sign. Examination of the terms in the shear stress evolution equation show that amplification of the pressure–strain correlation upon compression is responsible for this behavior.

The oblique angle between the directions of shear and compression is seen to significantly affect the response of sheared turbulence to compression. The effect of oblique angle on the evolution of kinetic energy may be explained by the initial distribution of $E_{\theta\theta}(\kappa_\theta)$ and $\overline{u_\theta^2}/q^2$, where θ is the direction of compression. Over a range of oblique angles varying from $-60°$ to $60°$ the amplification of $\overline{u_1^2}$, and q^2 is seen to decrease with increasing magnitude of oblique angle. Also, oblique compression reduces the tendency of

the shear stress to decrease in magnitude; for large oblique angles the shear stress amplifies.

The effect of initial anisotropy on turbulent kinetic energy evolution is verified in the compression of axisymmetric turbulence. The amplification of $\overline{u_1^2}$ of turbulence passed through a contraction is higher than that of isotropic turbulence—a result of having u_1 at lower κ_1. The amplification of q^2, on the other hand, is lower than that of isotropic turbulence—a result of a lower initial $\overline{u_1^2}/q^2$.

With respect to the shock/turbulence interaction, our results suggest that besides shock strength (defined in terms of the normal Mach number), the anisotropy of the turbulence and the shock inclination angle are important parameters in determining the evolution of turbulence across the shock. It is striking that the evolution of the Reynolds stresses upon oblique compression is qualitatively different for different oblique angles. These important effects of initial anisotropy and the shock inclination angle should be accounted for in the interpretation of experiments on the shock/turbulence interaction.

ACKNOWLEDGMENTS

This work was performed under AFOSR Grant No. 88-NA-322 monitored by Dr. L. Sakell. Computing resources provided by the NASA Ames Research Center and the NAS facility are greatly appreciated. We are thankful to Dr. S. Lee for many useful discussions and to Dr. P. Durbin for his comments on a draft of this manuscript. A shortened version of this paper was presented at the 31st Aerospace Sciences Meeting & Exhibit, 1993, Reno, Nevada.

[1]L. Prandtl, "Attaining a steady air stream in wind tunnels," NACA TN 726, 1933.
[2]G. I. Taylor, "Turbulence in a contracting stream," Z. Angew. Math. Mech. **15**, 91 (1935).
[3]H. S. Ribner and M. Tucker, "Spectrum of turbulence in a contracting stream," NACA TN 1113, 1953.
[4]G. K. Batchelor and I. Proudman, "The effect of rapid distortion of a fluid in turbulent motion," Q. J. Mech. Appl. Math. **7**, 83 (1954).
[5]M. J. Lee, "Distortion of homogeneous turbulence by axisymmetric strain and dilatation," Phys. Fluids A **1**, 1541 (1989).
[6]M. S. Uberoi, "Effect of wind-tunnel contraction on free-stream turbulence," J. Aeronaut. Sci. **23**, 754 (1956).
[7]A. J. Reynolds and H. J. Tucker, "The distortion of turbulence by general uniform irrotational strain," J. Fluid Mech. **68**, 673 (1975).
[8]M. J. Lee and W. C. Reynolds, "Numerical experiments on the structure of homogeneous turbulence," Report No. TF-24, Department of Mechanical Engineering, Stanford University, Stanford, CA, 1985.
[9]P. A. Durbin and O. Zeman, "Rapid distortion theory for homogeneous compressed turbulence with application to modeling," J. Fluid Mech. **242**, 349 (1992).
[10]C. Cambon, G. N. Coleman, and N. N. Mansour, "Rapid distortion analysis and direct simulation of compressible homogeneous turbulence at finite Mach number," in *Studying Turbulence Using Numerical Simulation Databases–IV*, Proceedings of the 1992 Summer Program (Center for Turbulence Research, Stanford, CA, 1992).
[11]G. N. Coleman and N. N. Mansour, "Modeling the rapid spherical compression of isotropic turbulence," Phys. Fluids A **3**, 2255 (1991).
[12]L. Jacquin, E. Blin, and P. Geffroy, "Experiments on free turbulence/shock wave interaction," *8th Symposium on Turbulent Shear Flows*, Munich, 1991 (Springer-Verlag, Berlin, 1991).
[13]A. A. Townsend, "The response of sheared turbulence to additional distortion," J. Fluid Mech. **81**, 171 (1980).
[14]K. R. Sreenivasan and R. Narasimha, "Rapid distortion of axisymmetric turbulence," J. Fluid Mech. **84**, 497 (1978).
[15]M. R. Maxey, "Distortion of turbulence in flows with parallel streamlines," J. Fluid Mech. **124**, 261 (1982).
[16]C. Cambon (private communication).
[17]A. M. Savill, "Recent developments in rapid distortion theory," Annu. Rev. Fluid Mech. **19**, 531 (1987).
[18]J. C. R. Hunt and D. J. Carruthers, "Rapid distortion theory and the 'problems' of turbulence," J. Fluid Mech. **242**, 497 (1990).
[19]J. R. A. Pearson, "The effect of uniform distortion on weak homogeneous turbulence," J. Fluid Mech. **5**, 274 (1959).
[20]R. G. Deissler, "Effect of inhomogeneity and of shear flow in weak turbulent fields," Phys. Fluids **4**, 1187 (1961).
[21]G. A. Blaisdell, N. N Mansour, and W. C. Reynolds, "Numerical simulations of compressible homogeneous turbulence," Report No. TF-50, Department of Mechanical Engineering, Stanford University, Stanford, CA, 1991.
[22]R. S. Rogallo, "Numerical experiments in homogeneous turbulence," NASA Tech. Memo 81315, 1981.
[23]H. K. Moffatt, "The interaction of turbulence with strong wind shear," in *Proceedings of the International Colloquium on Atmospheric Turbulence and Radio Wave Propagation*, Moscow, 1965, edited by A. M. Yaglom and V. I. Tatarsky (Nauka, Moscow, 1967), pp. 139–156.
[24]A. A. Townsend, "Entrainment and the structure of turbulent flow," J. Fluid Mech. **41**, 13 (1970).
[25]A. A. Townsend, *The Structure of Turbulent Shear Flow*, 2nd ed. (Cambridge U.P., Cambridge, 1976).
[26]P. Moin, "Similarity of organized structures in turbulent shear flows," in *Near-Wall Turbulence*, edited by S. J. Kline and N. H. Afgan (Hemisphere, New York, 1988), p. 2.
[27]M. J. Lee, J. Kim, and P. Moin, "Structure of turbulence at high shear rate," J. Fluid Mech. **216**, 561 (1990).